MOLECULAR AND CELLULAR BIOLOGY, May 2008, p. 3324–3335 Vol. 28, No. 10
0270-7306/08/$08.00+0 doi:10.1128/MCB.00144-08

Involvement of Actinin-4 in the Recruitment of JRAB/MICAL-L2 to Cell-Cell Junctions and the Formation of Functional Tight Junctions▽

Hiroyoshi Nakatsuji,[1,2] Noriyuki Nishimura,[1] Rie Yamamura,[1] Hiro-omi Kanayama,[2] and Takuya Sasaki[1]*

Departments of Biochemistry[1] and Urology,[2] Institute of Health Biosciences, The University of Tokushima Graduate School, Tokushima, Japan

Received 28 January 2008/Accepted 2 March 2008

Tight junctions (TJs) are cell-cell adhesive structures that undergo continuous remodeling. We previously demonstrated that Rab13 and a junctional Rab13-binding protein (JRAB)/molecule interacting with CasL-like 2 (MICAL-L2) localized at TJs and mediated the endocytic recycling of the integral TJ protein occludin and the formation of functional TJs. Here, we investigated how JRAB/MICAL-L2 was targeted to TJs. Using a series of deletion mutants, we found the plasma membrane (PM)-targeting domain within JRAB/MICAL-L2. We then identified actinin-4, which was originally isolated as an actin-binding protein associated with cell motility and cancer invasion/metastasis, as a binding protein for the PM-targeting domain of JRAB/MICAL-L2, using a yeast two-hybrid system. Actinin-4 was colocalized with JRAB/MICAL-L2 at cell-cell junctions and linked JRAB/MICAL-L2 to F-actin. Although actinin-4 bound to JRAB/MICAL-L2 without Rab13, the actinin-4–JRAB/MICAL-L2 interaction was enhanced by Rab13 activation. Depletion of actinin-4 by using small interfering RNA inhibited the recruitment of occludin to TJs during the Ca^{2+} switch. During the epithelial polarization after replating, JRAB/MICAL-L2 was recruited from the cytosol to cell-cell junctions. This JRAB/MICAL-L2 recruitment as well as the formation of functional TJs was delayed in actinin-4-depleted cells. These results indicate that actinin-4 is involved in recruiting JRAB/MICAL-L2 to cell-cell junctions and forming functional TJs.

Epithelial cells adhere tightly to one another to form epithelial sheets that separate different tissues and body compartments. Adhesion between epithelial cells is mediated by specialized intercellular junctional complexes, such as tight junctions (TJs) (1, 39, 51). TJs serve to form a selective barrier to diffusion through the intercellular space and to set the boundary between the apical and basolateral membrane domains of a cell. These junctions are composed of integral membrane proteins and cytoplasmic plaque proteins. The integral TJ proteins mediate cell-cell adhesion and include occludin, a large 24-member family of claudins, tricellulin, and junctional adhesion molecules. Although occludin was first identified as a component of TJ strands, claudins are now thought to constitute the backbones of these strands. Tricellulin, which was recently identified as another component of TJ strands, is specifically localized to the tricellular junctions (15). On the other hand, junctional adhesion molecules are thought to associate laterally with TJ strands (9). These integral TJ proteins bind and/or recruit TJ plaque proteins, which anchor the complexes to the actin cytoskeleton and serve as a scaffold for the recruitment of a variety of signaling proteins, including the Par-3/Par-6/atypical protein kinase C complex, the zonula occludens (ZO) proteins (ZO-1, ZO-2, and ZO-3), and membrane-associated guanylate kinase inverted (MAGI) proteins (MAGI-1, MAGI-2, and MAGI-3) (10, 44, 56).

Although TJs stably seal the intercellular space, they appear to be continuously remodeled within a confluent cultured epithelial monolayer (3, 30). Dynamic remodeling of TJs is controlled by the transport of integral TJ proteins to and/or from the plasma membrane (PM) (17). Rab family small G proteins play key roles in the regulation of intracellular membrane traffic (11, 36, 46, 57). Mammalian cells contain more than 63 different Rab family members that recognize distinct subsets of intracellular membranes. Rab proteins interconvert between GDP-bound and GTP-bound forms and thereby act as molecular switches. GDP/GTP exchange proteins (GEPs) and GTPase-activating proteins (GAPs) facilitate this interconversion by stimulating the release of bound GDP and the hydrolysis of bound GTP, respectively. Rab proteins also undergo a membrane association-and-dissociation cycle. GDP-bound Rab proteins in the cytosol are delivered to their target membranes, where Rab proteins are activated by GEP-stimulated GTP binding. In their GTP-bound forms, Rab proteins interact with a growing list of specific Rab effector proteins to carry out their diverse functions. Whereas Rab proteins regulate every step of vesicular transport, including vesicle budding, cytoskeleton-dependent motility, and vesicular tethering and fusion, it is thought that they also control the cytoskeleton-dependent motility of organelles and membrane-cytoskeleton interactions (20, 41, 43). Among the more than 63 Rab proteins, Rab13 was identified as a TJ plaque protein in epithelial cells and has been implicated in the assembly of functional TJs (27, 56). Rab13 also regulates neurite outgrowth and neuronal regeneration through the induction of p53 expression (7, 8).

In addition to the transport of integral TJ proteins to and/or from the PM, a dense band of actin and myosin that encircles epithelial cells at the level of TJs plays a crucial role in the

* Corresponding author. Mailing address: Department of Biochemistry, Institute of Health Biosciences, The University of Tokushima Graduate School, Tokushima 770-8503, Japan. Phone: 81-88-633-9223. Fax: 81-88-633-9227. E-mail: sasaki@basic.med.tokushima-u.ac.jp.

▽ Published ahead of print on 10 March 2008.

assembly and disassembly of TJs (16–18). The assembly of TJs occurs at the apical side of E-cadherin-mediated adherens junctions (AJs) in parallel with the maturation of spot-like primordial AJs into belt-like mature AJs (2, 47, 52). These processes require the precise spatiotemporal control of Rho family small G proteins, which are key regulators of actin dynamics. The activation of Rac1 and Arp2/3-dependent actin nucleation have been shown to be essential events in the assembly of TJs and AJs (4, 28). The mechanism underlying TJ disassembly also includes the reorganization of the perijunctional actomyosin ring, which results in the destabilization of *trans* interactions between integral TJ proteins of adjacent epithelial cells and the internalization of the TJ proteins. Accordingly, a growing number of actin-binding proteins, including ZO-1, ZO-2, and ZO-3 and Arp2/3, have been implicated in the assembly and disassembly of TJs (28).

The actinin proteins are a family of four closely related gene products that contain two calponin homology (CH) domains, four spectrin-like (SPEC) repeats, and two EF-hands (EFh) motifs (5, 34). Actinin-2 and actinin-3 are highly enriched in muscle, whereas actinin-1 and actinin-4 are expressed in many cell types. Actinin-2 and actinin-3 are major components of Z disks and dense bodies in striated and smooth muscle, whereas actinin-1 and actinin-4 are localized in stress fibers, cellular protrusions/leading edges, and cell adhesion sites in nonmuscle cells. Although the actinin proteins were initially described as actin cross-linking proteins in muscle, it is now clear that these proteins perform multiple roles in different cell types. For example, actinin anchors the myofibrillar actin filaments in muscle and is involved in anchoring the actin cytoskeleton to the PM in nonmuscle cells. Furthermore, actinin appears to serve as a scaffold that connects the actin cytoskeleton to a diverse range of cellular signaling pathways (34).

To begin to address the molecular mechanism of TJ remodeling, we previously reported that Rab13 regulates the endocytic recycling of occludin (29). Then, we identified a junctional Rab13-binding protein (JRAB)/molecule interacting with CasL-like 2 (MICAL-L2) as a novel Rab13 effector protein. Our results showed that JRAB/MICAL-L2, a large cytosolic protein that contains CH, LIM, and coiled-coil (CC) domains, localizes to TJs in polarized epithelial cells, is distributed along stress fibers in fibroblasts, and mediates the endocytic recycling of occludin and the formation of functional TJs (48). This protein belongs to the MICAL family of proteins including MICAL-1, MICAL-2, MICAL-3, MICAL-L1, and JRAB/MICAL-L2 (50). MICAL was originally identified as a binding protein for CasL/HEF1/NEDD9, which has been implicated in the regulation of the adhesive activities of integrins, the progression of the cell cycle, and the metastasis of melanoma (22, 37, 45). MICAL also functions in axon guidance downstream of the Sema3 receptor PlexA (50).

In the present study, we examined how JRAB/MICAL-L2 localized at TJs. We found a PM-targeting domain within JRAB/MICAL-L2 (JRAB/MICAL-L2-MN). We then identified actinin-4, which linked JRAB/MICAL-L2 to cell-cell junctions, as a JRAB/MICAL-L2-MN-binding protein.

MATERIALS AND METHODS

Plasmid construction. The mammalian expression vectors pCI-neo-HA-Rab13, pCI-neo-Myc-JRAB/MICAL-L2-F, and pCI-neo-Myc-JRAB/MICAL-L2-N have been described previously (48). Rab13, Rab13 T22N, and Rab13 Q67L cDNAs were subcloned from the pCI-neo-HA vector into the pCI-neo-Myc vector. JRAB/MICAL-L2-M (amino acids 261 to 805) and JRAB/MICAL-L2-MN (amino acids 261 to 679) cDNAs were generated by PCR using pCI-neo-Myc-JRAB/MICAL-L2-F as a template and cloned into the pCI-neo-Myc vector. JRAB/MICAL-L2-F (amino acids 1 to 1009) and JRAB/MICAL-L2-MN cDNAs were subcloned from the pCI-neo-Myc vector into the pCI-neo-HA vector. The MGC clone (clone no. 3157024) encoding mouse actinin-4 cDNA (NM_021895) was purchased from Invitrogen (Carlsbad, CA). Actinin-4-F (amino acids 1 to 912), actinin-4-N (amino acids 1 to 551), actinin-4-C (amino acids 552 to 912), actinin-4-CN (amino acids 552 to 736), and actinin-4-CC (amino acids 737 to 912) cDNAs were generated by PCR using an MGC clone (clone no. 3157024) as a template and cloned into the pCI-neo-Myc vector. All plasmids constructed in this study were sequenced using an ABI Prism 3100 genetic analyzer (Applied Biosystems, Foster City, CA).

Two-hybrid screening. JRAB/MICAL-L2-MN was cloned into the yeast two-hybrid bait vector pGBDU-C1 (19). A mouse 11-day-old embryo cDNA library in the yeast two-hybrid prey vector pACT2 was purchased from Clontech (Mountain View, CA). The yeast strain PJ69-4A (*MAT*a *trp1-901 leu2-3,112 ura3-52 his3-200 gal4*Δ *gal80*Δ *GAL2-ADE2 LYS2*::*GAL1-HIS3 met2*::*GAL7-lacZ*) was sequentially transformed with pGBDU-JRAB/MICAL-L2-MN and the mouse 11-day-old embryo cDNA library. Two-hybrid screening was performed and evaluated as described previously (19).

Antibodies. JRAB/MICAL-L2-C (amino acids 806 to 1009) cDNA was cloned into the pGEX-6P1 vector to express the N-terminal glutathione *S*-transferase (GST)-tagged JRAB/MICAL-L2-C protein. The GST and GST-JRAB/MICAL-L2-C fusion proteins were produced in *Escherichia coli* DH5α strain and purified using glutathione-Sepharose beads (GE Healthcare, Piscataway, NJ) according to the manufacturer's instructions. Two milligrams of GST or GST-JRAB/MICAL-L2-C protein was immobilized on HiTrap *N*-hydroxysuccinimide (NHS)-activated columns (GE Healthcare), according to the manufacturer's instructions. Two female Wistar rats were immunized with 100 μg of the GST-JRAB/MICAL-L2-C protein twice at 4-week intervals, after which whole blood was collected. Crude immunoglobulin fractions were prepared by ammonium sulfate precipitation and were passed through a GST-immobilized column to remove any anti-GST antibodies. The anti-JRAB/MICAL-L2 polyclonal antibody was purified further on a GST-JRAB/MICAL-L2-C-immobilized column according to the manufacturer's instructions. The rat antioccludin (MOC37) antibody was the kind gift of S. Tsukita (Kyoto University, Kyoto, Japan). Rat anti-E-cadherin was purchased from Takara (Otsu, Japan), rabbit anti-syntaxin 3 was from Synaptic Systems (Goettingen, Germany), rabbit anti-actinin-4 was from Alexis (Lausen, Switzerland), mouse anti-β-actin was from Sigma-Aldrich (St. Louis, MO), mouse anti-Myc (9E10) was from ATCC (Manassas, VA), mouse antihemagglutinin (HA) (clone 12CA5) and rat anti-HA (clone 3F10) were from Roche Diagnostics (Mannheim, Germany).

Cell culture and transfection. MTD-1A cells were kindly supplied by S. Tsukita (Kyoto University, Kyoto, Japan). Baby hamster kidney (BHK) cells were obtained from ATCC. MTD-1A and BHK cells were cultured at 37°C (in 5% CO_2 and 95% air) in Dulbecco's modified Eagle's medium with 10% fetal bovine serum and were transfected with the expression plasmid using a Nucleofector device (Amaxa, Köln, Germany) or Lipofectamine 2000 transfection reagent (Invitrogen) according to the manufacturers' instructions.

Western blots. Each sample was separated by sodium dodecyl sulfate (SDS)-polyacrylamide gel electrophoresis, and proteins were transferred to polyvinylidene difluoride membranes. Membrane blocking and antibody dilutions were done with a Block Ace (Dainippon Pharmaceutical, Osaka, Japan). Blots were developed by chemiluminescence using a horseradish peroxidase-coupled secondary antibody (Jackson ImmunoResearch Laboratories, West Grove, PA) with an ECL-Plus kit (GE Healthcare). Quantitation was performed with scans of autoradiograph films with nonsaturated signals, using ImageJ version 1.34 software (http://rsb.info.nih.gov/ij/).

Immunofluorescence microscopy. MTD-1A cells were grown on glass coverslips or filters and fixed with 2% formaldehyde in phosphate-buffered saline (PBS) at room temperature for 15 min. After cells were permeabilized with 0.2% Triton X-100 in PBS at room temperature for 15 min and blocked with 5% goat serum in PBS for 30 min, they were incubated with primary antibodies at room temperature for 45 min and then with Alexa 488- or Alexa 594-conjugated secondary antibodies (Invitrogen) for 45 min. F-actin was labeled with rhodamine-phalloidin (Invitrogen). Fluorescent images were acquired using a Radiance 2000 confocal laser scanning microscope (Bio-Rad, Hercules, CA).

Immunoprecipitation. To detect the actinin-4–JRAB/MICAL-L2 interaction, BHK and MTD-1A cells were lysed with lysis buffer containing 20 mM Tris-HCl (pH 7.5), 1.0% Triton X-100, 150 mM NaCl, 1 mM EDTA, and 20 μg/ml

(4-amidinophenyl)-methanesulfonyl fluoride (APMSF) at 4°C for 15 min. After an aliquot of the lysate was obtained, the remaining lysate was subjected to immunoprecipitation with anti-HA or anti-JRAB/MICAL-L2 antibody bound to protein G-Sepharose beads (GE Healthcare) and washed three times with wash buffer containing 20 mM Tris-HCl (pH 7.5), 1.0% Triton X-100, 150 mM NaCl, and 1 mM EDTA. The samples were then prepared for Western blotting analysis.

To detect the β-actin-actinin-4–JRAB/MICAL-L2 interaction, lysis buffer (5 mM Tris-HCl [pH 7.5], 1.0% Triton X-100, 2 mM $MgCl_2$, 100 mM KCl, 0.1 mM $CaCl_2$, 1 mM dithiothreitol, 0.2 mM ATP, and 20 μg/ml APMSF) and wash buffer (5 mM Tris-HCl [pH 7.5], 0.2% Triton X-100, and 100 mM KCl) were used.

To detect the actinin–4-JRAB/MICAL-L2 interaction in the presence of Rab13, lysis buffer {25 mM Tris-HCl [pH 7.5], 0.5% 3-[(3-cholamidopropyl)-dimethylammonio]-1-propanesulfonate [CHAPS], 125 mM NaCl, 5 mM EDTA, 6 mM $MgCl_2$, 20 μg/ml APMSF, and 100 μM GTPγS} and wash buffer (25 mM Tris-HCl [pH 7.5], 0.1% CHAPS, 300 mM NaCl, and 5 mM EDTA, 6 mM $MgCl_2$, and 10 μM GTPγS) were used.

To detect the actinin-4–JRAB/MICAL-L2 interaction in the presence of Rab13 T22N or Rab13 Q67L, lysis buffer (25 mM Tris-HCl [pH 7.5], 0.5% Triton X-100, 125 mM NaCl, 5 mM EDTA, 6 mM $MgCl_2$, and 20 μg/ml APMSF) and wash buffer (25 mM Tris-HCl [pH 7.5], 0.1% Triton X-100, 300 mM NaCl, 5 mM EDTA, and 6 mM $MgCl_2$) were used.

RNA interference. A 21-mer small interfering RNA (siRNA) duplex targeting mouse actinin-4 (GenBank/EMBL/DDBJ accession no. NM_021895 [5′-GGGAGAAGCAGCAGCGCAA-3′]), mouse JRAB/MICAL-L2 (GenBank/EMBL/DDBJ accession no. AB182579 [5′-GGCTGAAGCCTGTGGATAA-3′]), and a control nonsilencing RNA duplex, which did not match any known mouse gene, was obtained from B-Bridge (Sunnyvale, CA) and transfected into cells using a Nucleofector device according to the manufacturers' instructions.

Detergent solubility. To isolate the Triton X-100-soluble and -insoluble fractions, MTD-1A cells were lysed in 1.0% Triton X-100 buffer containing 20 mM Tris-HCl (pH 7.5), 100 mM NaCl, 5 mM EDTA, and 20 μg/ml APMSF. Lysates were incubated at 4°C for 15 min and then centrifuged at 15,000 × *g* at 4°C for 30 min. This supernatant was used as the Triton X-100-soluble fraction. The pellet was solubilized in 1% SDS buffer containing 20 mM Tris-HCl (pH 7.5), 100 mM NaCl, 5 mM EDTA, and 20 μg/ml APMSF, and used as the Triton X-100-insoluble fraction. Protein concentrations were determined using Bio-Rad protein assays (Bio-Rad) according to the manufacturer's instructions. Equal amounts of proteins were subjected to Western blotting analysis.

Replating of MTD-1A cells. Semiconfluent MTD-1A cells were dissociated into single cells by treating with 0.25% trypsin and 1 mM EDTA, and replated at a cell density necessary to obtain a nearly confluent monolayer. Cells were examined at 12, 24, 48, and 72 h after replating.

Ca^{2+} switch and quantitation of occludin length. A Ca^{2+}-switch assay and the acquisition of occludin images were performed as described previously (48). To quantify the mean occludin length per cell, the fields were randomly selected from fluorescent images containing more than 100 cells. The total occludin length at the cell-cell contact sites was measured using a Lumina Vision version 2.4 program (Mitani Corporation, Fukui, Japan), and the mean occludin length per cell was calculated by total occludin length/total cell number. Statistical analysis was performed using Student's *t* test.

Measurement of transepithelial electrical resistance (TER). MTD-1A cells were replated onto Transwell filters (a polycarbonate membrane with a 12-mm diameter and a 0.4-μm-pore size; Corning, Acton, MA), functioning as instant confluent monolayers, and cultured. The TER was measured directly from the culture medium at 0, 48, and 72 h after replating by using a Millicell electrical resistance system epithelial volt-ohm meter (Millipore, Billerica, MA). TER values were calculated by subtracting the background TER of blank filters and by multiplying the surface area of the filter.

RESULTS

JRAB/MICAL-L2 possesses the PM-targeting domain. To explore the molecular mechanism of JRAB/MICAL-L2 action, we first generated a series of JRAB/MICAL-L2 fragments, as follows: full-length JRAB/MICAL-L2 (JRAB/MICAL-L2-F; amino acids 1 to 1009), the N-terminal region of JRAB/MICAL-L2 containing the CH and LIM domains (JRAB/MICAL-L2-N; amino acids 1 to 805), the middle region of JRAB/MICAL-L2 between the LIM and CC domains (JRAB/MICAL-L2-M; amino acids 261 to 805), and the N-terminal region of JRAB/MICAL-L2-M (JRAB/MICAL-L2-MN; amino acids 261 to 679) (Fig. 1A). We then expressed Myc-tagged JRAB/MICAL-L2-F, JRAB/MICAL-L2-N, JRAB/MICAL-L2-M, and JRAB/MICAL-L2-MN in MTD-1A cells and examined their intracellular localizations by using immunofluorescence microscopy. As previously described (48), Myc-JRAB/MICAL-L2-F was targeted to the PM and perinuclear region, whereas Myc-JRAB/MICAL-L2-N was detected at the PM and in the nucleus (Fig. 1B, JRAB-F and JRAB-N). Deletion of the CH and LIM domains from JRAB/MICAL-L2-N did not affect its intracellular localization (Fig. 1B, JRAB-M). Interestingly, deletion of the 126 C-terminal amino acids from JRAB/MICAL-L2-M eliminated its nuclear localization and resulted in specific PM targeting (Fig. 1B, JRAB-MN). Together with our previous findings that the C-terminal region of JRAB/MICAL-L2 including the CC domain (amino acids 806 to 1009) interacted with Rab13 and localized to the cytosol (48), these results suggest that JRAB/MICAL-L2-MN is the primary PM-targeting domain within JRAB/MICAL-L2.

Actinin-4 binds to the PM-targeting domain of JRAB/MICAL-L2. Because JRAB/MICAL-L2-MN contained no recognizable membrane-interacting domains, we hypothesized that it may bind to another protein(s) that localized to the PM. Therefore, we screened a yeast two-hybrid library constructed from mouse 11-day-old embryo cDNA, using JRAB/MICAL-L2-MN as the bait. Three independent clones coding for proteins that specifically interacted with JRAB/MICAL-L2-MN were isolated. These positive clones contained sequences identical to actinin-4 cDNA (accession no. NM_021895). One of these prey clones encoded amino acids 552 to 912 of actinin-4 and specifically bound to JRAB/MICAL-L2-MN in the same two-hybrid assay (Fig. 2A). To confirm the yeast two-hybrid interactions between JRAB/MICAL-L2 and actinin-4 in intact cells, we performed coimmunoprecipitation experiments. For this purpose, we coexpressed Myc-tagged full-length actinin-4 (Myc-actinin-4-F; amino acids 1 to 912) with HA-JRAB/MICAL-L2-F in BHK cells. The lysate was subjected first to immunoprecipitation with anti-HA antibody bound to protein G-Sepharose beads. Then, the immunoprecipitates were subjected to Western blotting analysis using anti-Myc and anti-HA antibodies. Myc-actinin-4-F was specifically precipitated with HA-JRAB/MICAL-L2-F (Fig. 2B). The specific interaction between JRAB/MICAL-L2 and actinin-4 was also detected by reverse coimmunoprecipitation experiments (Fig. 2C). We next examined the interaction between JRAB/MICAL-L2 and actinin-4 in MTD-1A cells. When MTD-1A cell lysates were subjected to immunoprecipitation with anti-JRAB/MICAL-L2 antibody, endogenous actinin-4 was specifically precipitated with JRAB/MICAL-L2 (Fig. 2D). If JRAB/MICAL-L2 interacts with actinin-4 in the MTD-1A cells, the two molecules should colocalize at specific sites in the cells. When double-immunolabeling was performed with JRAB/MICAL-L2 and actinin-4 in MTD-1A cells grown on filters, JRAB/MICAL-L2 and actinin-4 primarily colocalized at cell-cell junctions (Fig. 2E). These results suggest that JRAB/MICAL-L2 is associated with actinin-4 at cell-cell junctions in MTD-1A cells.

Actinin-4 links JRAB/MICAL-L2 to F-actin. To further characterize the interaction between actinin-4 and JRAB/MICAL-L2, we first constructed Myc-tagged N-terminal actinin-4

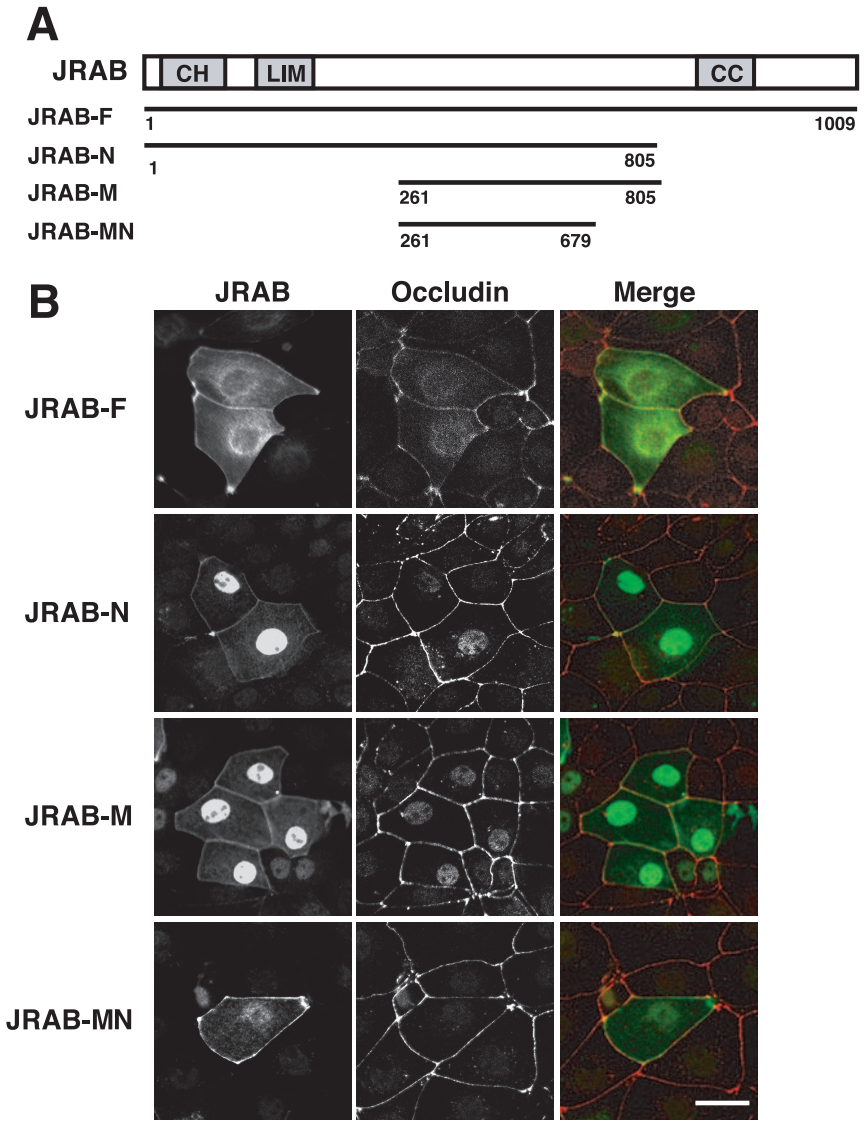

FIG. 1. Identification of the PM-targeting domain within JRAB/MICAL-L2. (A) Structures of the full-length and various fragments of JRAB/MICAL-L2. Numbers represent amino acid positions. CH, calponin homology domain; LIM, LIM domain; CC, coiled-coil domain. (B) MTD-1A cells were transfected with pCI-neo-Myc-JRAB/MICAL-L2-F, pCI-neo-Myc-JRAB/MICAL-L2-N, pCI-neo-Myc-JRAB/MICAL-L2-M, or pCI-neo-Myc-JRAB/MICAL-L2-MN and double immunolabeled with anti-Myc and anti-occludin antibodies. Bar, 20 μm. The results shown in panel B are representative of three independent experiments.

containing two CH domains and two SPEC repeats (Myc-actinin-4-N, amino acids 1 to 551) and C-terminal actinin-4 containing two SPEC repeats and two EFh motifs (Myc-actinin-4-C, amino acids 552 to 912) and tested their abilities to bind to JRAB/MICAL-L2-MN by immunoprecipitation (Fig. 3A). When Myc-actinin-4-F, Myc-actinin-4-N, and Myc-actinin-4-C were coexpressed with HA-JRAB/MICAL-L2-MN in BHK cells, Myc-actinin-4-F and Myc-actinin-4-C, but not Myc-actinin-4-N, specifically interacted with HA-JRAB/MICAL-L2-MN (Fig. 3B). We further divided actinin-4-C (amino acids 552 to 912) into actinin-4-CN containing two SPEC repeats (amino acids 552 to 736) and actinin-4-CC containing two EFh motifs (amino acids 737 to 912) and tested them for interactions with JRAB/MICAL-L2-MN (Fig. 3A). Whereas actinin-4-CC efficiently interacted with JRAB/MICAL-L2-MN, actinin-4-CN did not bind to this protein (Fig. 3B). Because actinin-4 binds to F-actin through its N-terminal CH domains, it may serve as a link between JRAB/MICAL-L2 and the actin cytoskeleton. To test this possibility, we examined the interaction between JRAB/MICAL-L2 and β-actin in the presence of actinin-4 by coimmunoprecipitation. Although β-actin did not directly associate with JRAB/MICAL-L2-F in BHK cells expressing HA-JRAB/MICAL-L2-F alone, the interaction between β-actin and JRAB/MICAL-L2 was clearly detected when Myc-actinin-4-F was coexpressed in these cells (Fig. 3C). These results suggested that actinin-4 links JRAB/MICAL-L2 to the actin cytoskeleton.

Rab13 activation enhances the actinin-4–JRAB/MICAL-L2 interaction. Because Rab13 was associated with JRAB/MICAL-L2 in a GTP-dependent manner (48), we investigated

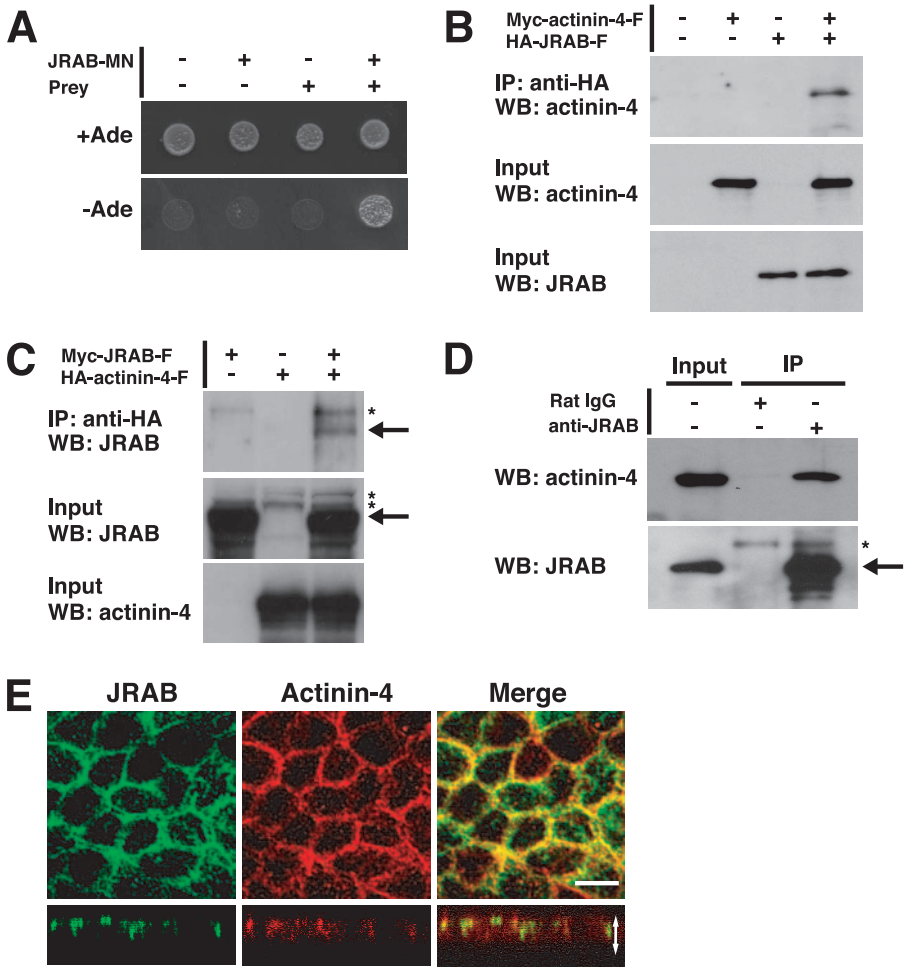

FIG. 2. Identification of actinin-4 as a binding protein for the PM-targeting domain of JRAB/MICAL-L2. (A) Yeast transformants carrying the pGBDU vector encoding JRAB/MICAL-L2-MN and the pACT2 vector encoding a prey clone were spotted onto synthetic complete medium lacking adenine to score for the *ADE2* reporter activity and incubated at 30°C for 3 days. (B and C) BHK cells cotransfected with pCI-neo-HA-JRAB/MICAL-L2 and pCI-neo-Myc-actinin-4 (B) or with pCI-neo-Myc-JRAB/MICAL-L2 and pCI-neo-HA-actinin-4 (C) were immunoprecipitated (IP) with anti-HA antibody and subjected to Western blotting (WB) analysis using anti-Myc and anti-HA antibodies. (D) MTD-1A cells were immunoprecipitated with anti-JRAB/MICAL-L2 antibody or rat immunoglobulin G and subjected to Western blotting analysis using anti-JRAB/MICAL-L2 and anti-actinin-4 antibodies. Arrows, Myc-JRAB and endogenous JRAB; asterisks, nonspecific bands. (E) MTD-1A cells grown on filters were double immunolabeled with anti-JRAB/MICAL-L2 and anti-actinin-4 antibodies and observed under a confocal microscope. Vertical sectional images are shown in the bottom panels. White arrow is equivalent in length to the thickness of the cellular sheet. Bar, 10 μm. The results shown in panels A to E are representative of three independent experiments.

whether JRAB/MICAL-L2 could simultaneously bind to both actinin-4 and Rab13. When Myc-actinin-4-F and HA-Rab13, with or without Myc-JRAB/MICAL-L2-F, were coexpressed in BHK cells, Myc-actinin-4 was specifically coimmunoprecipitated with HA-Rab13 in the presence of Myc-JRAB/MICAL-L2 (Fig. 4A), suggesting the existence of the actinin-4–JRAB/MICAL-L2-Rab13 complex. We next examined the effect of Rab13 activation on the actinin-4–JRAB/MICAL-L2 interaction. For this purpose, we generated a GTP binding mutant of Rab13 (Rab13 T22N) and a GTP hydrolysis mutant (Rab13 Q67L). When Myc-actinin-4-F and HA-JRAB/MICAL-L2-F were coexpressed with Myc-Rab13 T22N or Myc-Rab13 Q67L in BHK cells, the amount of Myc-actinin-4-F coimmunoprecipitated with HA-JRAB/MICAL-L2 was increased in the presence of Myc-Rab13 Q67L compared to that of Myc-Rab13 T22N (Fig. 4B). The effect of Rab13 activation on the actinin-4–JRAB/MICAL-L2 interaction was also detected by reverse coimmunoprecipitation experiments (Fig. 4C). If Rab13 activation enhanced the actinin-4–JRAB/MICAL-L2 interaction, the overexpression of wild-type Rab13 in the presence of GTPγS might have the same effect. When increased amounts of Myc-Rab13 were coexpressed with a constant amount of HA-JRAB/MICAL-L2 and Myc-actinin-4-F in BHK cells, the coexpression of Rab13 enhanced the actinin-4–JRAB/MICAL-L2 interaction in a dose-dependent manner (Fig. 4D). Although actinin-4 was able to interact with JRAB/MICAL-L2 without Rab13 as shown by the yeast two-hybrid assay and by immunoprecipitation (Fig. 2A and B), these results collectively suggested that the actinin-4–JRAB/MICAL-L2 interaction was enhanced by Rab13 activation.

Actinin-4 is involved in the recruitment of occludin to TJs during Ca^{2+} switch. We previously showed that the JRAB/

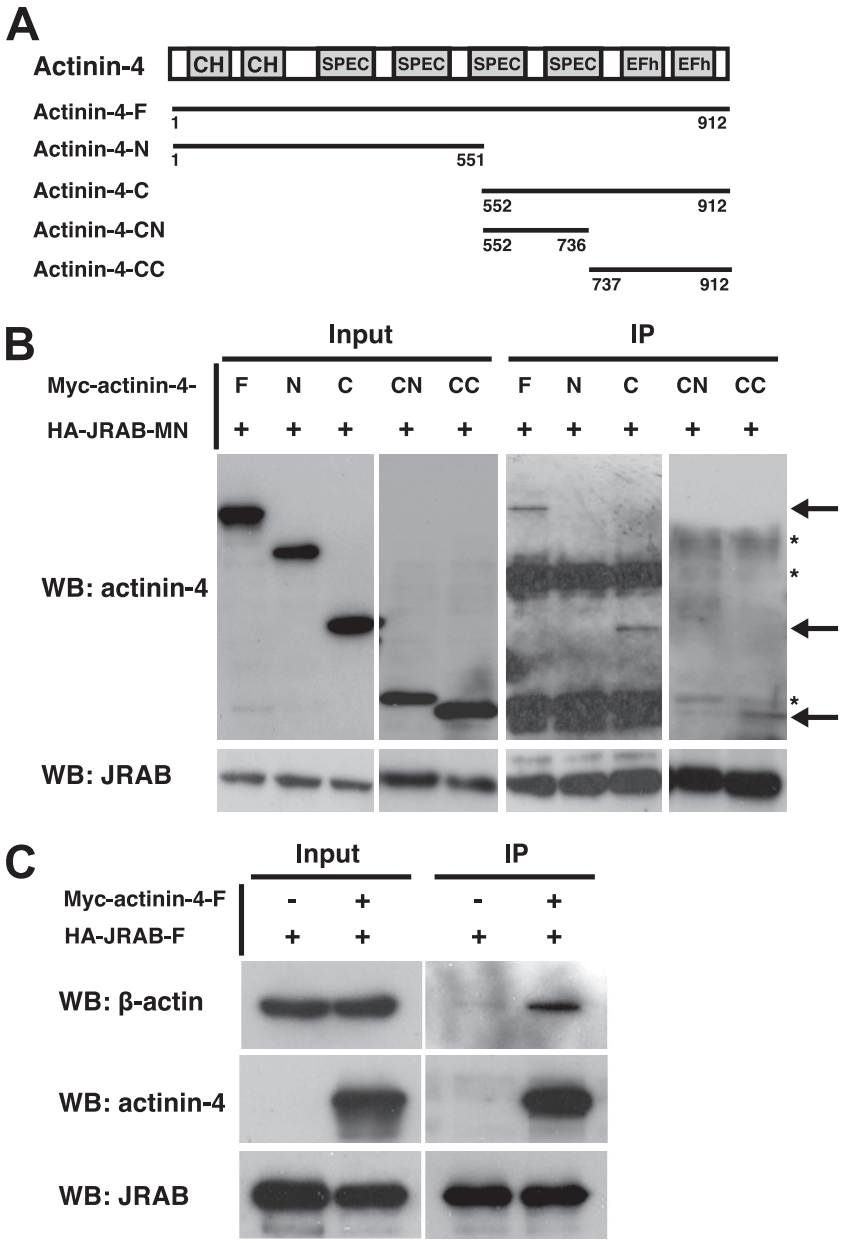

FIG. 3. Interaction of actinin-4 with JRAB/MICAL-L2 and F-actin. (A) Structures of the full-length and various fragments of actinin-4. Numbers represent amino acid positions. CH, calponin homology domain; SPEC, spectrin repeats; EFh, EF hands. (B) BHK cells cotransfected with pCI-neo-HA-JRAB/MICAL-L2-MN and pCI-neo-Myc-actinin-4-F, pCI-neo-Myc-actinin-4-N, pCI-neo-Myc-actinin-4-C, pCI-neo-Myc-actinin-4-CN, or pCI-neo-Myc-actinin-4-CC were immunoprecipitated (IP) with anti-HA antibody and subjected to Western blotting (WB) analysis using anti-Myc and anti-HA antibodies. Arrows indicate Myc-actinin-4-F, Myc-actinin-4-C, and Myc-actinin-4-CC, and asterisks indicate nonspecific bands. (C) BHK cells cotransfected with pCI-neo-HA-JRAB/MICAL-L2-F and pCI-neo-Myc-actinin-4-F were immunoprecipitated with anti-HA antibody and subjected to Western blotting analysis using anti-β-actin, anti-Myc, and anti-HA antibodies. The results shown in panels B and C are representative of three independent experiments.

MICAL-L2-Rab13 complex mediated the endocytic recycling of occludin and the formation of functional TJs (48). This prompted us to examine the role of actinin-4 in the endocytic recycling of occludin by using a well-established Ca^{2+}-switch model. For this purpose, we designed siRNA that targeted mouse actinin-4 (accession no. NM_021895) and transfected it into MTD-1A cells. Compared to the control RNA, actinin-4 siRNA suppressed the expression of the actinin-4 protein in MTD-1A cells (Fig. 5A). When actinin-4-depleted cells were stained with antibodies specific for the apical marker (syntaxin 3) and the basolateral marker (E-cadherin), these markers were distributed normally and were well differentiated from each other (Fig. 5B) (26, 31). Control and actinin-4-depleted MTD-1A cells were first incubated in Ca^{2+}-chelated medium to dissociate cell-cell junctions and were then cultured in a physiological Ca^{2+} medium to induce the assembly of cell-cell

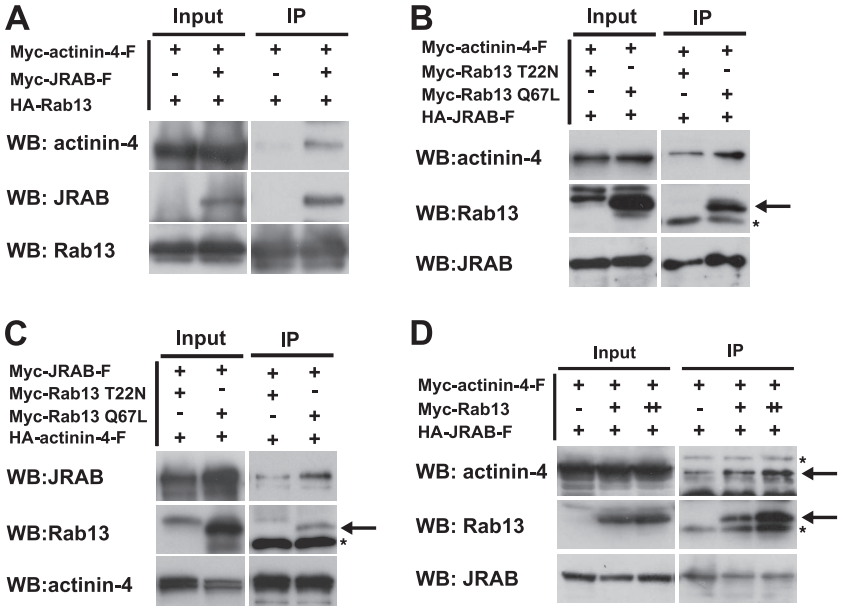

FIG. 4. Involvement of Rab13 activation in the regulation of the actinin-4–JRAB/MICAL-L2 interaction. BHK cells cotransfected with pCI-neo-HA-Rab13 and pCI-neo-Myc-actinin-4-F together with pCI-neo-Myc or pCI-neo-Myc-JRAB/MICAL-L2 (A), with pCI-neo-HA-JRAB/MICAL-L2 and pCI-neo-Myc-actinin-4-F together with pCI-neo-Myc-Rab13 T22N or pCI-neo-Myc-Rab13 Q67L (B), with pCI-neo-HA-actinin-4-F and pCI-neo-Myc-JRAB/MICAL-L2 together with pCI-neo-Myc-Rab13 T22N or pCI-neo-Myc-Rab13 Q67L (C) or with pCI-neo-HA-JRAB/MICAL-L2 (+, 1.5 μg) and pCI-neo-Myc-actinin-4-F (+, 3.0 μg) together with pCI-neo-Myc (−, 3.0 μg), pCI-neo-Myc plus pCI-neo-Myc-Rab13 (+, 1.5 plus 1.5 μg), or pCI-neo-Myc-Rab13 (++, 3.0 μg) (D) were immunoprecipitated (IP) with an anti-HA antibody and subjected to Western blotting (WB) analysis using anti-HA and anti-Myc antibodies. Arrows indicate Myc-Rab13 and Myc-actinin-4, and asterisks indicate nonspecific bands. The results shown in panels A to D are representative of three independent experiments.

junctions. Similar to the inhibition of Rab13 and JRAB/MICAL-L2 function (48), the depletion of actinin-4 slowed the kinetics of occludin recruitment to TJs at 4 and 6 h after Ca^{2+} restoration (Fig. 5C and D). These results suggested that actinin-4 was involved in the recruitment of occludin to TJs during the Ca^{2+} switch in MTD-1A cells.

Actinin-4 is involved in the recruitment of JRAB/MICAL-L2 to cell-cell junctions during Ca^{2+} switch. As actinin-4 bound to the PM-targeting domain of JRAB/MICAL-L2, we next examined the role of actinin-4 in the PM targeting of JRAB/MICAL-L2, using a Ca^{2+}-switch model. Although JRAB/MICAL-L2 was not a transmembrane protein like occludin, it was gradually recruited and accumulated to cell-cell junctions at 6 h after Ca^{2+} restoration in control MTD-1A cells (Fig. 6A). In contrast to that of control cells, this JRAB/MICAL-L2 recruitment was impaired in actinin-4-depleted cells at 4 and 6 h after Ca^{2+} restoration (Fig. 6A). As actinin-4 formed the complex with JRAB/MICAL-L2 and was localized to cell-cell junctions, JRAB/MICAL-L2 could also regulate the localization of actinin-4. To test this possibility, we knocked down JRAB/MICAL-L2 in MTD-1A cells and performed a Ca^{2+}-switch assay. When JRAB/MICAL-L2 siRNA was transfected into MTD-1A cells, the expression of JRAB/MICAL-L2 was efficiently knocked down compared to that of control RNA-transfected cells (Fig. 6B). Like JRAB/MICAL-L2, the time-dependent appearance and accumulation of actinin-4 at cell-cell junctions were observed during the 6-h Ca^{2+} restoration in control MTD-1A cells (Fig. 6C). Although the actinin-4 at cell-cell junctions seemed slightly less concentrated in JRAB/MICAL-L2-depleted cells, its appearance was similar to that of control cells (Fig. 6C). While we cannot formally exclude the possible involvement of JRAB/MICAL-L2 in determining the localization of actinin-4 at present, these results suggested that actinin-4 was involved in the recruitment of JRAB/MICAL-L2 to cell-cell junctions during Ca^{2+} switch in MTD-1A cells.

JRAB/MICAL-L2 is recruited from the cytosol to the cell-cell junctions during epithelial polarization after replating. Although JRAB/MICAL-L2 is a cytosolic protein, it was detected in both the cytosolic and membrane/cytoskeleton fractions after subcellular fractionation of MTD-1A cells (48). Because JRAB/MICAL-L2 was localized primarily at TJs in polarized MTD-1A cells, we hypothesized that it may be recruited from the cytosol to TJs during the epithelial polarization process. To test this possibility, we examined the intracellular distribution of JRAB/MICAL-L2 during MTD-1A cell polarization after replating (2, 55). Semiconfluent MTD-1A cells were dissociated into single cells and then replated on glass coverslips under confluent conditions. At 12, 24, 48, and 72 h after replating, the cells were labeled with anti-JRAB/MICAL-L2 antibody together with rhodamine-phalloidin to visualize the actin filaments. Twelve hours after cells were replated, JRAB/MICAL-L2 was distributed mainly in the cytosol. It was then gradually recruited to cell-cell junctions within 72 h after replating (Fig. 7A). This was paralleled by the development of the perijunctional actin belt (Fig. 7A). Because nonionic detergent insolubility is considered to be an indicator of protein incorporation into cytoskeleton-associated junctional complexes (38), we next examined the Triton X-100 insolubility of JRAB/MICAL-L2 during MTD-1A cell polarization after replating. For this purpose, we treated MTD-1A

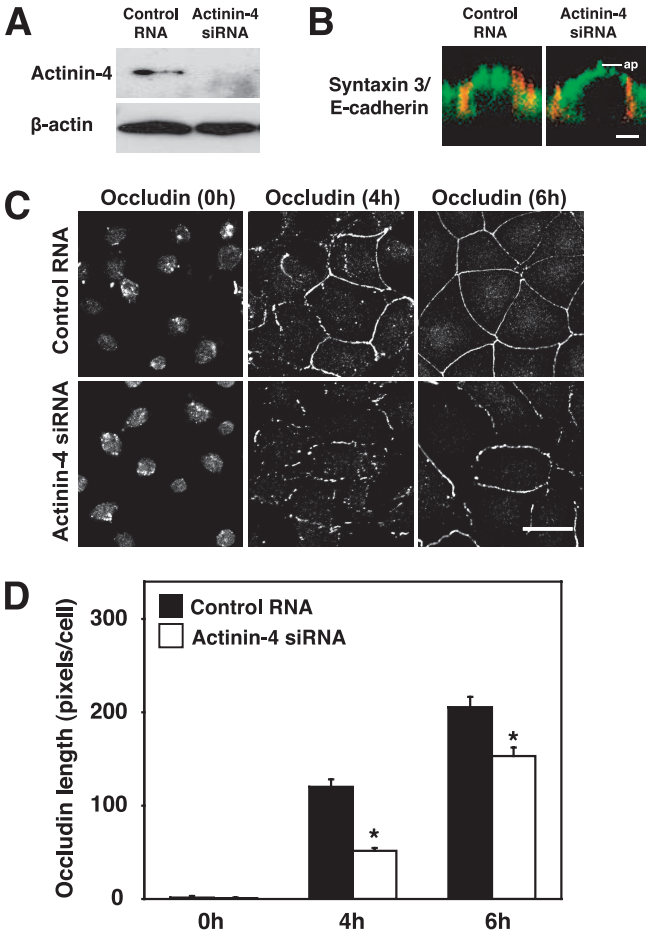

FIG. 5. Involvement of actinin-4 in the recruitment of occludin to TJs during the Ca^{2+} switch. (A) MTD-1A cells were transfected with control RNA or with actinin-4 siRNA and subjected to Western blotting analysis using anti-actinin-4 and anti-β-actin antibodies. (B) MTD-1A cells transfected with control RNA or actinin-4 siRNA were double immunolabeled for apical markers (syntaxin 3, green) and basolateral markers (E-cadherin, red). Bar, 5 μm. ap, level of the apical membranes. (C) MTD-1A cells transfected with control RNA or actinin-4 siRNA were subjected to a Ca^{2+}-switch assay and then immunostained with antioccludin antibody at 0, 4, and 6 h after Ca^{2+} restoration. Bar, 20 μm. The results shown in panels A to C are representative of three independent experiments. (D) Occludin length per cell was quantitated and shown as the means and standard errors of the means of three independent experiments. Asterisks denote significant differences from control cells ($P < 0.05$).

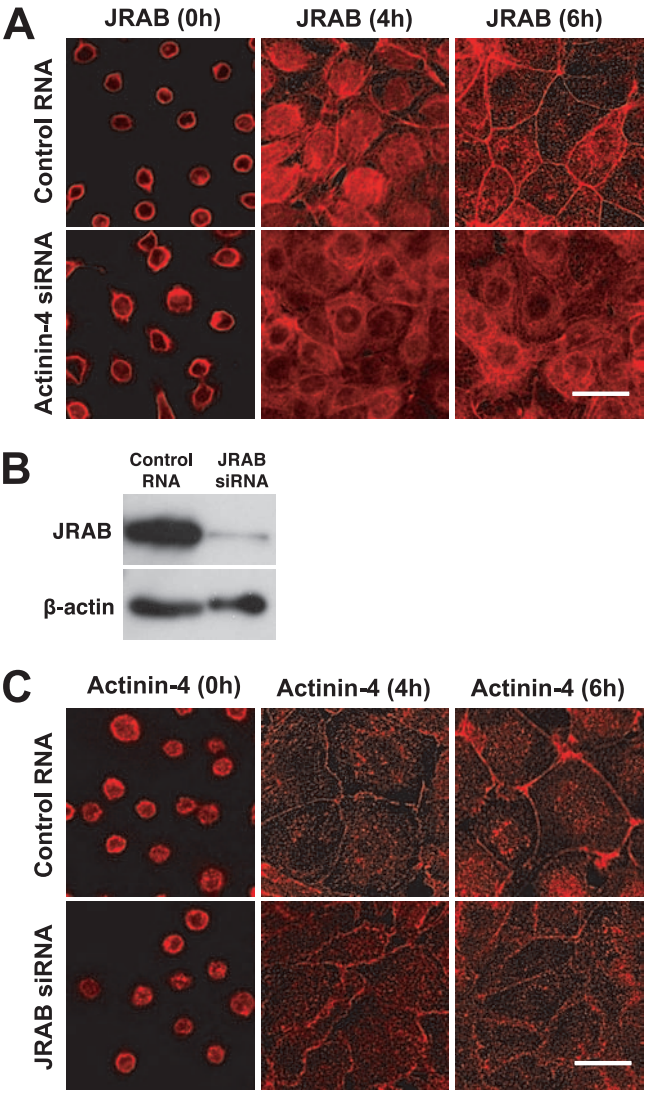

FIG. 6. Involvement of actinin-4 in the recruitment of JRAB/MICAL-L2 to the cell-cell junctions during the Ca^{2+} switch. (A) MTD-1A cells transfected with control RNA or actinin-4 siRNA were subjected to a Ca^{2+}-switch assay and then immunostained with anti-JRAB/MICAL-L2 antibody at 0, 4, and 6 h after Ca^{2+} restoration. Bar, 20 μm. (B) MTD-1A cells were transfected with control RNA or JRAB/MICAL-L2 siRNA and subjected to Western blotting analysis using anti-JRAB/MICAL-L2 and anti-β-actin antibodies. (C) MTD-1A cells transfected with control RNA or JRAB/MICAL-L2 siRNA were subjected to a Ca^{2+}-switch assay and then immunostained with anti-actinin-4 antibody at 0, 4, and 6 h after Ca^{2+} restoration. Bar, 20 μm. The results shown in panels A to C are representative of three independent experiments.

cells with 1.0% Triton X-100 and prepared the Triton X-100-soluble and -insoluble fractions at 12, 24, 48, and 72 h after they were replated. In accordance with the morphological data (Fig. 7A), the level of JRAB/MICAL-L2 detected in the Triton X-100-insoluble fractions was gradually increased after replating (Fig. 7B and C). These results indicated that JRAB/MICAL-L2 was recruited from the cytosol to the cell-cell junctions during MTD-1A cell polarization.

Actinin-4 is involved in the recruitment of JRAB/MICAL-L2 to cell-cell junctions and the formation of functional TJs during epithelial polarization after replating. We next examined the role of actinin-4 in the recruitment of JRAB/MICAL-L2 to the cell-cell junctions during MTD-1A cell polarization. In control MTD-1A cells, JRAB/MICAL-L2 was localized to the cytosol at 12 h after replating and was then recruited to the cell-cell junctions within 72 h (Fig. 8A). The level of JRAB/MICAL-L2 recruitment to the cell-cell junctions, however, was lower in actinin-4-depleted cells than in the control cells at 24 and 48 h after replating (Fig. 8A). To complement the morphological data, we then investigated the nonionic detergent insolubility of JRAB/MICAL-L2 at 12, 24, 48, and 72 h after replating. When we treated control MTD-1A cells with 1.0%

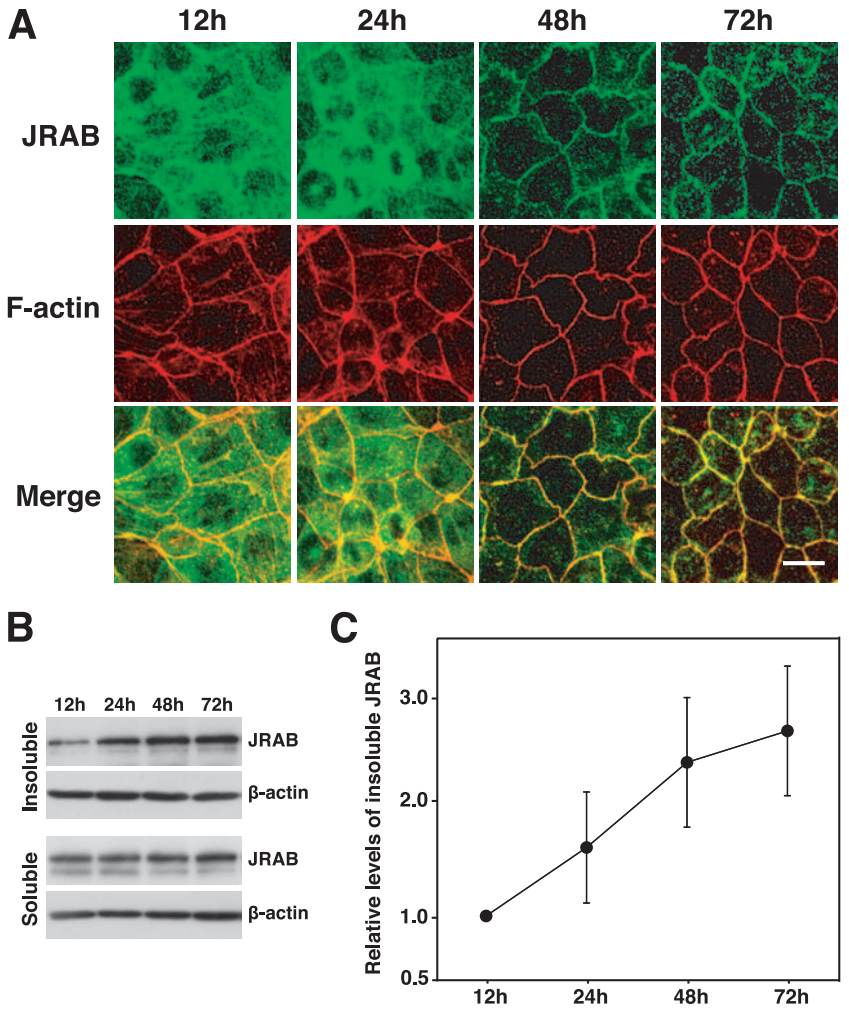

FIG. 7. Recruitment of JRAB/MICAL-L2 from the cytosol to the cell-cell junctions during epithelial polarization after replating. (A) MTD-1A cells were dissociated into single cells, replated under confluent conditions, cultured for the indicated times, and then double labeled with rhodamine-phalloidin and anti-JRAB/MICAL-L2 antibody. Bar, 10 μm. The results shown are representative of three independent experiments. (B) Triton X-100-soluble and -insoluble fractions were prepared from MTD-1A cells cultured for the indicated times after replating. Equal amounts of proteins were subjected to Western blotting analysis using anti-JRAB/MICAL-L2 and anti-β-actin antibodies. (C) The levels of insoluble JRAB/MICAL-L2 protein were calculated as protein level at the indicated time/protein level at 12 h and shown as the means and standard errors of the means of three independent experiments.

Triton X-100, the amounts of JRAB/MICAL-L2 detected in the Triton X-100-insoluble fractions were gradually increased from 12 h to 72 h after replating (Fig. 8B). In contrast, the Triton X-100-insoluble JRAB/MICAL-L2 extracted from the actinin-4-depleted MTD-1A cells did not increase (Fig. 8B). We further assessed the role of actinin-4 in the development of TER, which is often used to monitor the barrier function of TJs during MTD-1A cell polarization. MTD-1A cells transfected with control RNA or actinin-4 siRNA were dissociated into single cells and were then replated onto filters as an instant confluent monolayer. TER was then measured at 0, 48, and 72 h after replating. When we followed the development of TER in MTD-1A cells transfected with control RNA, we noticed a decrease in the maximal TER (>1,000 Ω cm^2) even in MTD-1A cells that were subjected to the transfection procedure without RNA, using a Nucleofector device. Under this experimental condition, actinin-4-depleted cells exhibited a substantially delayed increase in TER compared to that of control MTD-1A cells (Fig. 8C). These results suggested that actinin-4 was involved in the recruitment of JRAB/MICAL-L2 to cell-cell junctions and the formation of functional TJs during MTD-1A cell polarization.

DISCUSSION

The remodeling of TJs is essential for epithelial cells to acquire defined shapes and assemble into ordered structures during development (40). The transport of integral TJ proteins to and/or from the PM provides a key regulatory mechanism for TJ remodeling (18). We previously found that Rab13 and its effector protein JRAB/MICAL-L2 were colocalized at TJs in polarized epithelial cells and regulated the endocytic recycling of occludin and the formation of functional TJs (29, 48). In the present study, we examined how JRAB/MICAL-L2 lo-

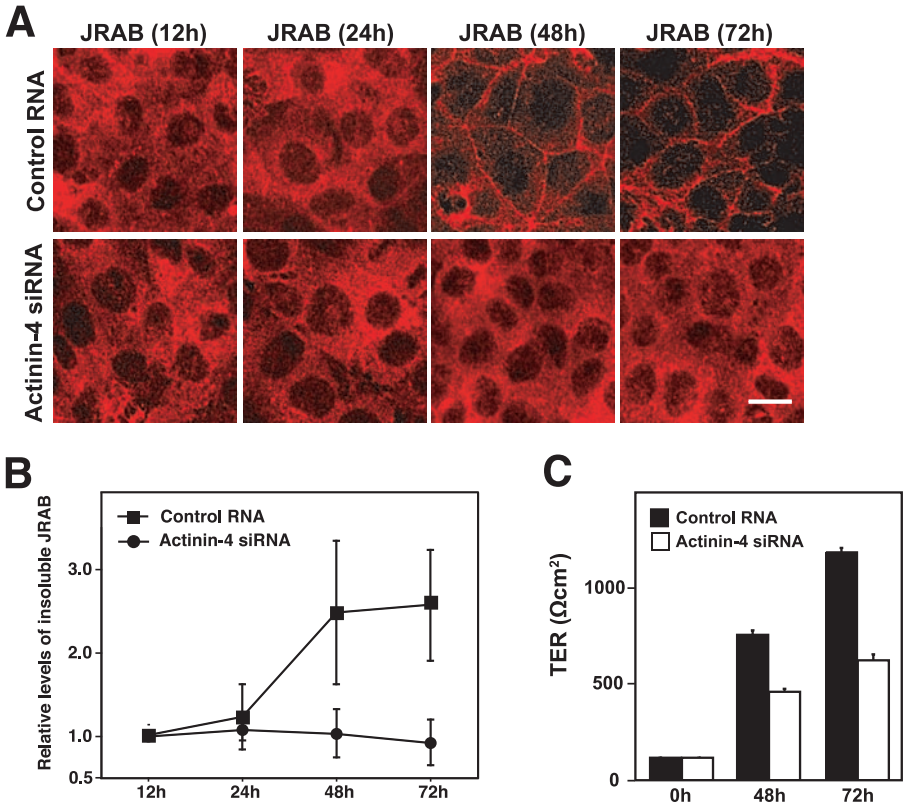

FIG. 8. Involvement of actinin-4 in the recruitment of JRAB/MICAL-L2 to the cell-cell junctions and the formation of functional TJs during epithelial polarization after replating. (A) MTD-1A cells transfected with control RNA or actinin-4 siRNA were dissociated into single cells, replated under confluent conditions, cultured for the indicated times, and then immunolabeled with anti-JRAB/MICAL-L2 antibody. Bar, 10 μm. The results shown are representative of three independent experiments. (B) Triton X-100-soluble and -insoluble fractions were prepared from MTD-1A cells transfected with control RNA or actinin-4 siRNA and cultured for the indicated times after replating. Equal amounts of proteins were subjected to Western blotting analysis using anti-JRAB/MICAL-L2 antibody. The levels of insoluble JRAB/MICAL-L2 protein were calculated as protein level at the indicated time/protein level at 12 h and are shown as the means and standard errors of the means of three independent experiments. (C) MTD-1A cells transfected with control RNA or actinin-4 siRNA were replated onto Transwell filters as an instant confluent monolayer and cultured. TER was measured at 0, 48, and 72 h after replating, and values are shown as the means and standard errors of the means of three independent experiments.

calized at TJs. Our results have produced four key findings. First, the middle region of JRAB/MICAL-L2 targets the protein to the PM, and the protein was recruited from the cytosol to the cell-cell junctions during epithelial polarization. Second, actinin-4 bound to the PM-targeting domain of JRAB/MICAL-L2 and linked JRAB/MICAL-L2 to F-actin. Third, the actinin-4–JRAB/MICAL-L2 interaction was enhanced by Rab13 activation. Fourth, actinin-4 was involved in the recruitment of occludin to TJs, the recruitment of JRAB/MICAL-L2 to the cell-cell junctions, and the formation of functional TJs.

Because JRAB/MICAL-L2 did not possess the transmembrane and membrane interaction domains, it is likely to be linked to the cytoplasmic face of the transmembrane protein(s) or the membrane anchoring protein(s). Using a series of JRAB/MICAL-L2 deletion mutants, we were able to locate the PM-targeting domain in a 419-amino-acid region between the LIM and CC domains. To our surprise, the PM-targeting domain of JRAB/MICAL-L2 did not contain the CH and LIM domains, both of which are important for protein-protein interactions and are found in a number of membrane-anchoring proteins. When we assessed the Triton X-100 insolubility of JRAB/MICAL-L2, it gradually increased during epithelial polarization, which requires a complex interplay between the assembly of AJs and TJs, the activation of evolutionarily conserved polarity protein complexes, the redistribution of organelles, the polarization of membrane traffic, and the reorganization of actin and microtubule cytoskeletons (32). Interestingly, the kinetics of JRAB/MICAL-L2 recruitment to the cell-cell junctions were slower than the formation of the circumferential actin belt, whereas they were correlated with the development of TER, suggesting that JRAB/MICAL-L2 might act at a later stage of epithelial polarization.

In the present study, we identified actinin-4 as a binding protein for the PM-targeting domain of JRAB/MICAL-L2. Consistent with our previous results showing that JRAB/MICAL-L2 colocalized with F-actin and potentially linked Rab13 to the actin cytoskeleton to mediate the formation of functional TJs (48), actinin-4 colocalized with JRAB/MICAL-L2 at cell-cell junctions and linked JRAB/MICAL-L2 to β-actin. In agreement with our data, actinin-4 has been linked to cell-cell junctions. In epithelial cells, actinin-4 associates with β-catenin at AJs (13) and with MAGI-1 and ZO-1 at TJs (6, 35). In glomerular epithelial cells (podocytes), mutations in the actinin-4 gene are shown to cause the dysfunction

of slit diaphragm (SD), a junctional structure that links the interdigitating foot processes from neighboring podocytes and contains features of both AJs and TJs, and lead to focal and segmental glomerulosclerosis, which is characterized by progressive proteinuria and podocyte foot process effacement (21, 24). Interestingly, in parallel with epithelial TJs, where actinin-4 associates with ZO-1, MAGI-1, and the Rab13 effector protein JRAB/MICAL-L2 (6, 35), actinin-4 has been identified in the integral SD protein nephrin complex containing MAGI-2 and the Rac1/Cdc42 effector protein IQGAP1 (25).

Although actinin-4 is broadly expressed and likely acts at a variety of cell-cell junctions, actinin-4-deficient mice showed abnormalities only in the kidneys and developed severely damaged podocytes and progressive glomerular disease (23). In addition to the kidney-specific phenotype of actinin-4-deficient mice, the tissue-specific regulation of actinin-4 function is suggested by several cancers. While elevated actinin-4 expression mediates tumor progression of colorectal and non-small lung cell cancers, the tumor suppressive effect of actinin-4 is observed with neuroblastoma and prostate cancer cells (12, 14, 33, 53). Although the molecular mechanism for the lack of widespread epithelial dysfunction outside the kidneys remains elusive, highly homologous actinin-1 and/or many actinin-4-binding proteins are expected to play an important role in compensating for the actinin-4 deficiency outside of the kidneys in vivo. Interestingly, we found that JRAB/MICAL-L2 can associate with actinin-1 (data not shown), and the significance of the actinin-1–JRAB/MICAL-L2 interaction is currently under investigation.

Recent evidence has indicated that actinin-4 is involved in the endocytic recycling processes. Actinin-4 has been shown to interact with clathrin and dynamin, which can mediate the clathrin-dependent endocytosis from the PM (12). The actinin-4-Hrs-BERP-myosin V complex is required for the efficient recycling of the transferrin receptor (TfR) (54), and the expression of actinin-4 affects the recycling of TfR in prostate cancer cells (12). Here, we described the interaction of actinin-4 with JRAB/MICAL-L2, which mediated the endocytic recycling of occludin but not TfR (48). Although we do not currently know the exact role of actinin-4 in these complexes, the two actinin-4 complexes may act at distinct steps during endocytic recycling within a cell. For example, the actinin-4-Hrs-BERP-myosin V complex residing at the recycling endosomes facilitates the myosin V-dependent TfR transport to the PM (54), whereas the actinin-4–JRAB/MICAL-L2-Rab13 complex residing at the cell-cell junctions specifically regulates occludin transport to the PM (48).

Dynamic polymerization and depolymerization of F-actin and myosin-dependent translocation of actin filaments provide the potential mechanisms for TJ remodeling (28). Recent studies suggested that F-actin reorganization results in the destabilization of *trans* interactions between integral TJ proteins of adjacent epithelial cells and thereby triggers an internalization of the TJ proteins. In calcium-depleted T84 intestinal epithelial cells, the disruption of E-cadherin-mediated adhesion triggers the selective early formation of contractile actomyosin rings, which induce the endocytosis of occludin and claudins (16). Latrunculin A-induced actin depolymerization in MDCK cells causes a rapid disruption of TJ barriers, which coincides with the endocytosis of occludin but not of claudins (42). In support of the potential role of actinin-4 in these TJ remodeling processes, actinin-4 was identified as one of the gene products that was upregulated by Rac1 and Cdc42 (49), which are key regulators of TJ remodeling and epithelial polarization. Although further studies are required to elucidate the relationship between the actinin-4–JRAB/MICAL-L2-Rab13 complex and the TJ remodeling processes, it is clear that epithelial cells coordinate a number of signals to dynamically reorganize TJs in physiological and pathological conditions.

In summary, the present study demonstrates that JRAB/MICAL-L2 associates with actinin-4 at cell-cell junctions in polarized epithelial cells and is recruited from the cytosol to the cell-cell junctions during epithelial polarization. Actinin-4 is involved in the recruitment of JRAB/MICAL-L2 to the cell-cell junctions and the formation of functional TJs.

ACKNOWLEDGMENTS

We thank S. Tsukita (Kyoto University, Kyoto, Japan) for the anti-occludin (MOC37) antibody and MTD-1A cells.

This study was supported by Grants-in-Aid for Scientific Research (18590271to N.N. and 15079207 and 18390089 to T.S.) from the Ministry of Education, Culture, Sports, Science, and Technology of Japan.

REFERENCES

1. **Anderson, J., C. Van Itallie, and A. Fanning.** 2004. Setting up a selective barrier at the apical junction complex. Curr. Opin. Cell Biol. **16:**140–145.
2. **Ando-Akatsuka, Y., S. Yonemura, M. Itoh, M. Furuse, and S. Tsukita.** 1999. Differential behavior of E-cadherin and occludin in their colocalization with ZO-1 during the establishment of epithelial cell polarity. J. Cell Physiol. **179:**115–125.
3. **Bertet, C., L. Sulak, and T. Lecuit.** 2004. Myosin-dependent junction remodelling controls planar cell intercalation and axis elongation. Nature **429:**667–671.
4. **Braga, V., and A. Yap.** 2005. The challenges of abundance: epithelial junctions and small GTPase signalling. Curr. Opin. Cell Biol. **17:**466–474.
5. **Broderick, M., and S. Winder.** 2005. Spectrin, α-actinin, and dystrophin. Adv. Protein Chem. **70:**203–246.
6. **Chen, V., X. Li, H. Perreault, and J. Nagy.** 2006. Interaction of zonula occludens-1 (ZO-1) with α-actinin-4: application of functional proteomics for identification of PDZ domain-associated proteins. J. Proteome Res. **5:**2123–2134.
7. **Di Giovanni, S., A. De Biase, A. Yakovlev, T. Finn, J. Beers, E. Hoffman, and A. Faden.** 2005. *In vivo* and *in vitro* characterization of novel neuronal plasticity factors identified following spinal cord injury. J. Biol. Chem. **280:**2084–2091.
8. **Di Giovanni, S., C. Knights, M. Rao, A. Yakovlev, J. Beers, J. Catania, M. Avantaggiati, and A. Faden.** 2006. The tumor suppressor protein p53 is required for neurite outgrowth and axon regeneration. EMBO J. **25:**4084–4096.
9. **Ebnet, K., A. Suzuki, S. Ohno, and D. Vestweber.** 2004. Junctional adhesion molecules (JAMs): more molecules with dual functions? J. Cell Sci. **117:**19–29.
10. **Gonzalez-Mariscal, L., A. Betanzos, P. Nava, and B. Jaramillo.** 2003. Tight junction proteins. Prog. Biophys. Mol. Biol. **81:**1–44.
11. **Grosshans, B., D. Ortiz, and P. Novick.** 2006. Rabs and their effectors: achieving specificity in membrane traffic. Proc. Natl. Acad. Sci. USA **103:**11821–11827.
12. **Hara, T., K. Honda, M. Shitashige, M. Ono, H. Matsuyama, K. Naito, S. Hirohashi, and T. Yamada.** 2007. Mass spectrometry analysis of the native protein complex containing actinin-4 in prostate cancer cells. Mol. Cell Proteomics **6:**479–491.
13. **Hayashida, Y., K. Honda, M. Idogawa, Y. Ino, M. Ono, A. Tsuchida, T. Aoki, S. Hirohashi, and T. Yamada.** 2005. E-cadherin regulates the association between β-catenin and actinin-4. Cancer Res. **65:**8836–8845.
14. **Honda, K., T. Yamada, Y. Hayashida, M. Idogawa, S. Sato, F. Hasegawa, Y. Ino, M. Ono, and S. Hirohashi.** 2005. Actinin-4 increases cell motility and promotes lymph node metastasis of colorectal cancer. Gastroenterology **128:**51–62.
15. **Ikenouchi, J., M. Furuse, K. Furuse, H. Sasaki, S. Tsukita, and S. Tsukita.** 2005. Tricellulin constitutes a novel barrier at tricellular contacts of epithelial cells. J. Cell Biol. **171:**939–945.
16. **Ivanov, A., I. McCall, C. Parkos, and A. Nusrat.** 2004. Role for actin filament turnover and a myosin II motor in cytoskeleton-driven disassembly of the epithelial apical junctional complex. Mol. Biol. Cell **15:**2639–2651.

17. **Ivanov, A., D. Hunt, M. Utech, A. Nusrat, and C. Parkos.** 2005. Differential roles for actin polymerization and a myosin II motor in assembly of the epithelial apical junctional complex. Mol. Biol. Cell **16:**2636–2650.
18. **Ivanov, A., A. Nusrat, and C. Parkos.** 2005. Endocytosis of the apical junctional complex: mechanisms and possible roles in regulation of epithelial barriers. Bioessays **27:**356–365.
19. **James, P., J. Halladay, and E. Craig.** 1996. Genomic libraries and a host strain designed for highly efficient two-hybrid selection in yeast. Genetics **144:**1425–1436.
20. **Jordens, I., M. Marsman, C. Kuijl, and J. Neefjes.** 2005. Rab proteins, connecting transport and vesicle fusion. Traffic **6:**1070–1077.
21. **Kaplan, J., S. Kim, K. North, H. Rennke, L. Correia, H. Tong, B. Mathis, J. Rodríguez-Pérez, P. Allen, A. Beggs, and M. Pollak.** 2000. Mutations in ACTN4, encoding α-actinin-4, cause familial focal segmental glomerulosclerosis. Nat. Genet. **24:**251–256.
22. **Kim, M., J. Gans, C. Nogueira, A. Wang, J. Paik, B. Feng, C. Brennan, W. Hahn, C. Cordon-Cardo, S. Wagner, T. Flotte, L. Duncan, S. Granter, and L. Chin.** 2006. Comparative oncogenomics identifies NEDD9 as a melanoma metastasis gene. Cell **125:**1269–1281.
23. **Kos, C., T. Le, S. Sinha, J. Henderson, S. Kim, H. Sugimoto, R. Kalluri, R. Gerszten, and M. Pollak.** 2003. Mice deficient in α-actinin-4 have severe glomerular disease. J. Clin. Investig. **111:**1683–1690.
24. **Lee, D., E. Huang, and H. Ward.** 2006. Tight junction biology and kidney dysfunction. Am. J. Physiol. Renal Physiol. **290:**F20–34.
25. **Lehtonen, S., J. Ryan, K. Kudlicka, N. Iino, H. Zhou, and M. Farquhar.** 2005. Cell junction-associated proteins IQGAP1, MAGI-2, CASK, spectrins, and α-actinin are components of the nephrin multiprotein complex. Proc. Natl. Acad. Sci. USA **102:**9814–9819.
26. **Low, S., S. Chapin, T. Weimbs, L. Kömüves, M. Bennett, and K. Mostov.** 1996. Differential localization of syntaxin isoforms in polarized Madin-Darby canine kidney cells. Mol. Biol. Cell **7:**2007–2018.
27. **Marzesco, A., I. Dunia, R. Pandjaitan, M. Recouvreur, D. Dauzonne, E. Benedetti, D. Louvard, and A. Zahraoui.** 2002. The small GTPase Rab13 regulates assembly of functional tight junctions in epithelial cells. Mol. Biol. Cell **13:**1819–1831.
28. **Mege, R., J. Gavard, and M. Lambert.** 2006. Regulation of cell-cell junctions by the cytoskeleton. Curr. Opin. Cell Biol. **18:**541–548.
29. **Morimoto, S., N. Nishimura, T. Terai, S. Manabe, Y. Yamamoto, W. Shinahara, H. Miyake, S. Tashiro, M. Shimada, and T. Sasaki.** 2005. Rab13 mediates the continuous endocytic recycling of occludin to the cell surface. J. Biol. Chem. **280:**2220–2228.
30. **Nagafuchi, A., S. Ishihara, and S. Tsukita.** 1994. The roles of catenins in the cadherin-mediated cell adhesion: functional analysis of E-cadherin-α catenin fusion molecules. J. Cell Biol. **127:**235–245.
31. **Nelson, W., R. Hammerton, A. Wang, and E. Shore.** 1990. Involvement of the membrane-cytoskeleton in development of epithelial cell polarity. Semin. Cell Biol. **1:**359–371.
32. **Nelson, W.** 2003. Adaptation of core mechanisms to generate cell polarity. Nature **422:**766–774.
33. **Nikolopoulos, S., B. Spengler, K. Kisselbach, A. Evans, J. Biedler, and R. Ross.** 2000. The human non-muscle α-actinin protein encoded by the ACTN4 gene suppresses tumorigenicity of human neuroblastoma cells. Oncogene **19:**380–386.
34. **Otey, C., and O. Carpen.** 2004. α-Actinin revisited: a fresh look at an old player. Cell Motil. Cytoskeleton **58:**104–111.
35. **Patrie, K., A. Drescher, A. Welihinda, P. Mundel, and B. Margolis.** 2002. Interaction of two actin-binding proteins, synaptopodin and α-actinin-4, with the tight junction protein MAGI-1. J. Biol. Chem. **277:**30183–30190.
36. **Pfeffer, S., and D. Aivazian.** 2004. Targeting Rab GTPases to distinct membrane compartments. Nat. Rev. Mol. Cell Biol. **5:**886–896.
37. **Pugacheva, E., and E. Golemis.** 2005. The focal adhesion scaffolding protein HEF1 regulates activation of the Aurora-A and Nek2 kinases at the centrosome. Nat. Cell Biol. **7:**937–946.
38. **Sakakibara, A., M. Furuse, M. Saitou, Y. Ando-Akatsuka, and S. Tsukita.** 1997. Possible involvement of phosphorylation of occludin in tight junction formation. J. Cell Biol. **137:**1393–1401.
39. **Schneeberger, E., and R. Lynch.** 2004. The tight junction: a multifunctional complex. Am. J. Physiol. Cell Physiol. **286:**C1213–1228.
40. **Schock, F., and N. Perrimon.** 2002. Molecular mechanisms of epithelial morphogenesis. Annu. Rev. Cell Dev. Biol. **18:**463–493.
41. **Seabra, M., and E. Coudrier.** 2004. Rab GTPases and myosin motors in organelle motility. Traffic **5:**393–399.
42. **Shen, L., and J. Turner.** 2005. Actin depolymerization disrupts tight junctions via caveolae-mediated endocytosis. Mol. Biol. Cell **16:**3919–3936.
43. **Soldati, T., and M. Schliwa.** 2006. Powering membrane traffic in endocytosis and recycling. Nat. Rev. Mol. Cell Biol. **7:**897–908.
44. **Suzuki, A., and S. Ohno.** 2006. The PAR-aPKC system: lessons in polarity. J. Cell Sci. **119:**979–987.
45. **Suzuki, T., T. Nakamoto, S. Ogawa, S. Seo, T. Matsumura, K. Tachibana, C. Morimoto, and H. Hirai.** 2002. MICAL, a novel CasL interacting molecule, associates with vimentin. J. Biol. Chem. **277:**14933–14941.
46. **Takai, Y., T. Sasaki, and T. Matozaki.** 2001. Small GTP-binding proteins. Physiol. Rev. **81:**153–208.
47. **Takai, Y., and H. Nakanishi.** 2003. Nectin and afadin: novel organizers of intercellular junctions. J. Cell Sci. **116:**17–27.
48. **Terai, T., N. Nishimura, I. Kanda, N. Yasui, and T. Sasaki.** 2006. JRAB/MICAL-L2 is a junctional Rab13-binding protein mediating the endocytic recycling of occludin. Mol. Biol. Cell **17:**2465–2475.
49. **Teramoto, H., R. Malek, B. Behbahani, M. Castellone, N. Lee, and J. Gutkind.** 2003. Identification of H-Ras, RhoA, Rac1 and Cdc42 responsive genes. Oncogene **22:**2689–2697.
50. **Terman, J., T. Mao, R. Pasterkamp, H. Yu, and A. Kolodkin.** 2002. MICALs, a family of conserved flavoprotein oxidoreductases, function in plexin-mediated axonal repulsion. Cell **109:**887–900.
51. **Tsukita, S., M. Furuse, and M. Itoh.** 2001. Multifunctional strands in tight junctions. Nat. Rev. Mol. Cell Biol. **2:**285–293.
52. **Vasioukhin, V., C. Bauer, M. Yin, and E. Fuchs.** 2000. Directed actin polymerization is the driving force for epithelial cell-cell adhesion. Cell **100:**209–219.
53. **Yamagata, N., Y. Shyr, K. Yanagisawa, M. Edgerton, T. Dang, A. Gonzalez, S. Nadaf, P. Larsen, J. Roberts, J. Nesbitt, R. Jensen, S. Levy, J. Moore, J. Minna, and D. Carbone.** 2003. A training-testing approach to the molecular classification of resected non-small cell lung cancer. Clin. Cancer Res. **9:**4695–4704.
54. **Yan, Q., W. Sun, P. Kujala, Y. Lotfi, T. Vida, and A. Bean.** 2005. CART: an Hrs/actinin-4/BERP/myosin V protein complex required for efficient receptor recycling. Mol. Biol. Cell **16:**2470–2482.
55. **Yonemura, S., M. Itoh, A. Nagafuchi, and S. Tsukita.** 1995. Cell-to-cell adherens junction formation and actin filament organization: similarities and differences between non-polarized fibroblasts and polarized epithelial cells. J. Cell Sci. **108:**127–142.
56. **Zahraoui, A., G. Joberty, M. Arpin, J. Fontaine, R. Hellio, A. Tavitian, and D. Louvard.** 1994. A small rab GTPase is distributed in cytoplasmic vesicles in non polarized cells but colocalizes with the tight junction marker ZO-1 in polarized epithelial cells. J. Cell Biol. **124:**101–115.
57. **Zerial, M., and H. McBride.** 2001. Rab proteins as membrane organizers. Nat. Rev. Mol. Cell Biol. **2:**107–117.